THE PUBLISHING HOUSE
OF THE ROMANIAN ACADEMY

PROCEEDINGS OF THE ROMANIAN ACADEMY, Series A,
Volume 20, Number 2/2019, pp. 169–178

MODELLING OF SOLAR PHOTOVOLTAIC ARRAY FED BRUSHLESS DC MOTOR DRIVE USING ENHANCED DC-DC CONVERTER

Sathish KUMAR SHANMUGAM[1], Karthikeyan MUTHUSAMY[2], Vijayachitra CHENNIPPAN[2], Suresh BALASUBRAMANIAM[3], Sampathkumar RAMASAMY[3], Saravanan SUBRAMANIAN[1]

[1] Jansons Institute of Technology, Coimbatore, Tamilnadu, India
[2] Kongu Engineering College, Erode, Tamilnadu, India
[3] KPR Institute of Engineering and Technology, Coimbatore, Tamilnadu, India
Corresponding author: Sathish Kumar SHANMUGAM, E-mail: ssk@jit.ac.in

Abstract. The proposed research involves modeling of solar photovoltaic array fed BLDC Drive using enhanced DC-DC converter. Both step-up and step-down converter, DC-link unit are proposed in this research. The proposed circuit includes modern feed-forward sensing methods for applied potential Sensing, Third harmonic Voltage combination, Terminal Current Sensing, Back-EMF Integration and PWM strategies. For the efficiency improvement reduced number of switches in the proposed circuit makes the scheme more outlay efficient and the motor speed is synchronized by PI controller as a result it is more efficient compared with conventional. The recent techniques based on analysis and values, models are clearly experimented in the research. A Matlab platform and hardware model of two-output output Buck-Boost converter is developed and its concert is analysed for various effective environment.

Key words: TOBB, losses, DC-DC converter, ripple voltage, simulation.

1. INTRODUCTION

With an impressive increase in energy utilization in recent decades, ecological hitches like pollution are widespread in global and energy saving technology requires greater attention. Renewable energy sources and the electrifying drive, i.e., electrical machines need to be pollution-free and highly capable energy transmission devices with low blare quality are required to solve the energy consumption problem. Brushless Direct Current Motor (BLDC) is employed for increasing the efficiency of torque production because it has no brushes in addition to features over conventional motors like eradication of ionizing sparks from the commutator, increment in power and overall reduction in Electromagnetic interference (EMI). It also has improved Speed and torque characteristics, more effectiveness and dependability, long existence and soundless performance. In general, BLDC is highly capable of converting electricity into mechanical power than Brushed DC motors. This enhancement is largely because of absence of electrical and friction losses. In addition, the control of BLDC is quiet easy compare to AC motors [1]. Since, due to brushes, control to load and torque to current ratios of AC and DC motors are high. One of the smartest applications for photovoltaic (PV) energy consumption technique is solar water pumping system driven by an electric motor. The overheads of PV equipment and water pumps are likely to dwindle more over the next few years so it is no conjecture that the demand for the PV power gets increased. As a result PV water pumping systems will become more economic in the near future [2-3]. In isolated areas, PV water pumping systems are popularly utilized to meet household energy demand and also pumped water for irrigation, common agriculture purpose, day to day requirements. The advantages of using PV based water pumps include low maintenance, ease of installation, reliability and matching between the presence of the PV power and the need for water usage. In modern days, the BLDC plays a vital role in automotive applications especially on Electric Vehicle(EV) and fuel pumps due to its high efficiency, compact size and low maintenance when compared to a brush DC motor[4-5]. To obtain an accurate and harmonics-free instantaneous torque of BLDC, the rotor position information for stator current commutation must be known, which can be obtained using hall sensors mounted on a rotor [6-8].

2. MATERIALS AND METHODS

PV energy is becoming one of the most popular renewable energies, but, with the varying ecological conditions like temperature and solar irradiation, the PV characteristics curve is inconsistent in MPPT, thus imposing a challenge to the solar tracking issue. The situation becomes more complex when the array is treated with partial shading, i.e., a condition where a portion or the entire module of the PV array is not uniform insolation [9-10]. The sudden variation in solar insolation leads to the reduction in the rated solar power, and as a consequence, the focus is on the battery backup powered system in order to meet the load requirement in motor drives. Moreover the efficient BB converter is necessary for the gratifying operational. To fulfill this requirement, B6-Inverter is reconfigured into a four-switch three phase inverter (B4-Inverter), due to reconfiguration of inverter, in case of a switch/leg failure and reduce the cost and system size is also currently given an increasing attention [11-15].

2.1. Objectives of the proposed research

The main objectives of the present research are as below: 1) To design a enhanced Buck-Boost converter for operation in discontinuous conduction for improving the life time of the battery. 2) To design a Two-output output enhanced BB converter for employing B4-inverter. 3) To improve the efficiency of the enhanced BB converter highly. 4) To reduce the current conduction losses by designing the Enhanced BB converter with minimal number of components. 5) To regulate the load voltage with high quality in all power flow situations, by using three-domain load voltage control method. 6) To validate the performance of the proposed enhance BB converter for employing it in commercial applications.

2.2. Design of standalone two-output buck-boost converter fed B4-inverter and single-stage PV -battery powered BLDC drive

The switching state, switch (S_1) is ON, the diode (D_2) gets forward biased so switch (S_2) is turned ON/OFF. The equivalent circuit of proposed the converter is illustrated in Fig. 2. In state of switching input DC source (V_{in}) charges the inductor (L_1), and hence the inductor current increase. At time, intermediate capacitor (C_1) and input dc source (V_{in}) delivers/discharges its energy to the output capacitor (C_{O2}) through diode (D_2). In addition, in this mode, capacitors (C_{01} and C_{O2}) get discharged to the motor, as illustrated in Fig. 2. The current and the voltage of the inductor and capacitors are expressed as in Equations (1)-(3) below,

$$L_1 \frac{\mathrm{d}i_{L1}}{\mathrm{d}t} = -V_{c1} \tag{1}$$

$$C_{01} \frac{\mathrm{d}V_{01}}{\mathrm{d}t} = -\frac{V_{01}}{R_1} \tag{2}$$

$$C_{O2}\,\mathrm{d}V_{O2} = V_{c1} + V_{in} - V_{O2}. \tag{3}$$

2.2.1. Proposed converter modes of operation

Mode 0. When switch (S_2) is in "ON" condition and switch (S_1) is in "OFF" condition, current in inductance (L_1) drops (discharging). As a result, the intermediary capacitor (C_1) gets (charging) energy from an input inductor (L_1). Consequently, voltage across the intermediary capacitor C_1 boosts as given in Fig. 1b.

Mode 1. When switch (S_1) is in "ON" condition, current in supply voltage drops (discharging). Consequently, the energy is transmitted to the inductance (L_1) (charging). Therefore, voltage across the intermediary capacitor C_1 boosts as given in Fig. 1b. Simultaneously, current in the capacitor C_1 and the supply current V_{dc} drops (discharging). As a result, the energy is transmitted to the capacitor (C_{O2}) (charging) with the help of diode D_2. Consequently, voltage across the intermediary capacitor C_{O2} boosts as given in Fig. 1c.

Mode 2. When switches (S_1) and (S_2) is in "OFF" condition, current in inductance (L_1) drops (discharging). As a result, the intermediary capacitor (C_1) gets (charging) energy from input inductor (L_1) with the help the diode D_1.

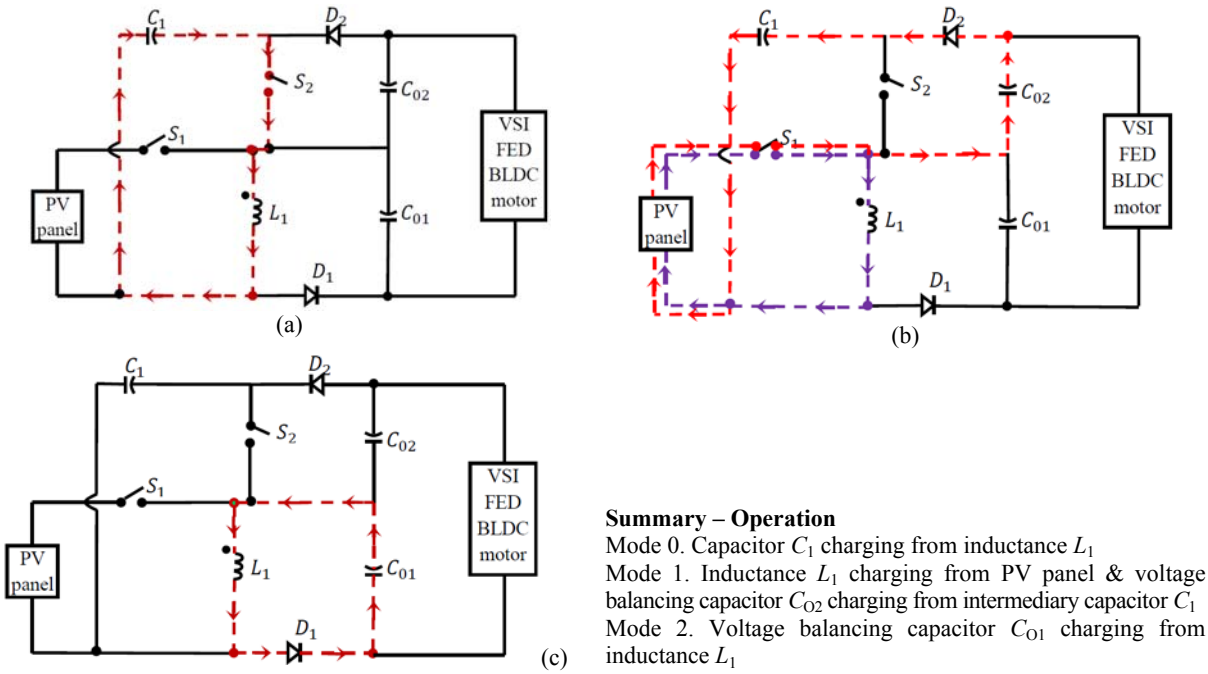

Summary – Operation
Mode 0. Capacitor C_1 charging from inductance L_1
Mode 1. Inductance L_1 charging from PV panel & voltage balancing capacitor C_{O2} charging from intermediary capacitor C_1
Mode 2. Voltage balancing capacitor C_{O1} charging from inductance L_1

Fig. 1 – Modes of operation.

The involvement of current research depends on the TOBB converter by selecting a Proportional Integral (PI) controller for a closed loop control strategy. The PI controller computation has two unique modes: proportional mode and integral mode.

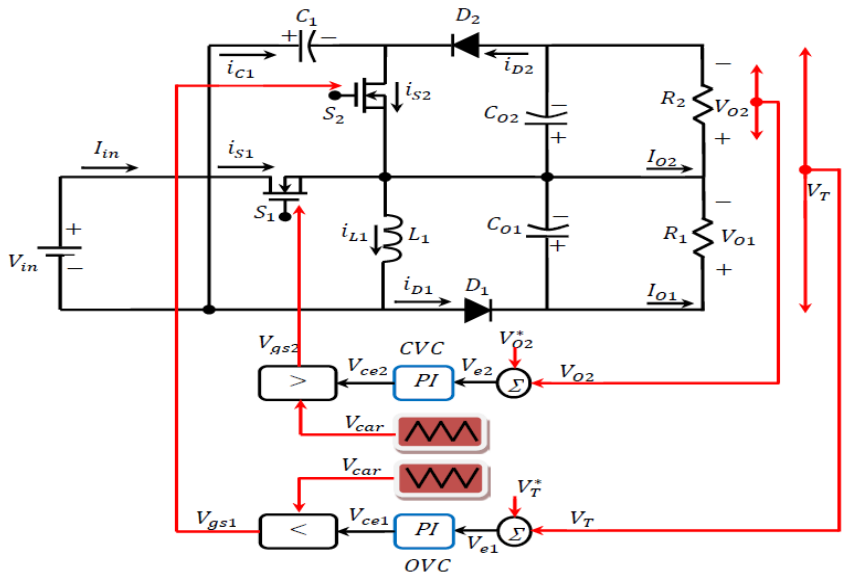

Fig. 2 – Control of TOBB converter.

The two modes provide the output in accurate action to the control element. PI controller is used in industries due to its simple design and unrefined arrangement. PI controller algorithm can be run by Eq. (4)

$$Output(t) = K_P\, err(t) + K_I \int_0^t err(t)\,\mathrm{d}t \tag{4}$$

where means $err(t)$ = set voltage – actual voltage.

As observed from Fig. 2 the control strategy of TOBB converter, OVC compares of the output voltage (V^*_{out}) of TOBB converter with original output voltage (V_{out}) for generates error voltage (V_{ce1}), provided. The

error generator of CVC compares the TOBB converter capacitor (C_{01}) voltage (V_{01}^{*}) with output voltage (V_{01}) and produce an error voltage (V_{ce2}).

2.2.2. Losses on switch $S_{1,2}$ during conduction

Losses on Switch $S_{1,2}$ during conduction**,** the circuit is simplified to be a precise voltage drop which in series with linear resistor (R_{DS} on=0.07). R_{DS} on is based on the applied V_{GS} and the junction temperature. The losses on switch $S_{1,2}$ during conduction $S_{1,2}$ is expressed in Equations (5) and (6)

$$P_{\text{cond}-S2} = I_{S_{1,2}}^2 \cdot \text{RDS}_{\text{on}} \tag{5}$$

$$I_{S_{1,2}}^2 = D_2 \cdot \left[I_{\text{OS}_{1,2}}^2 + \frac{I_{\text{OS}_{1,2}}^2}{12} \right] \tag{6}$$

where ($I_{S_{1,2}}$) indicates the current curving during the switch ($S_{1,2}$), (D_2) stands for the "ON" time of switch (S_2). Switching current at the beginning instant (I_{OS_2}) is derived from Equation (7)

$$I_{\text{OS}_{1,2}} = I_{\text{OS}_{1,2}-\text{min}} + \Delta I_{\text{OS}_{1,2}} = 7.565. \tag{7}$$

Harmonics current ($\Delta I_{OS_{1,2}}$) are given as in Equation (8)

$$\Delta I_{\text{OS}_{1,2}} = \frac{I_{\text{OS}_{1,2}-\text{max}} - I_{\text{OS}_{1,2}-\text{min}}}{2} = \frac{8.53 - 6.6}{2} = 0.965. \tag{8}$$

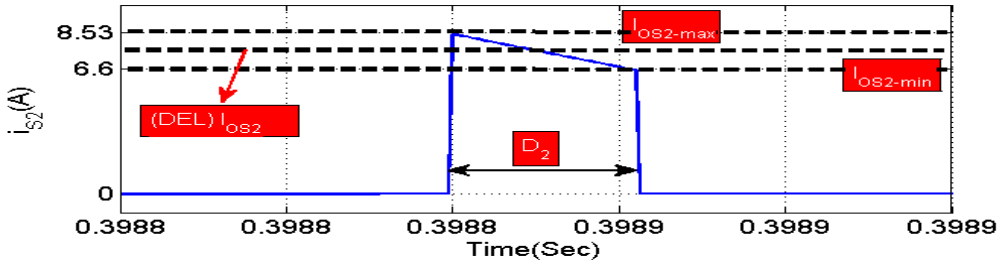

Fig. 3 – Open loop waveform during switch ($S_{1,2}$) conduction.

($I_{OS_{1,2}-\text{max}}$) and ($I_{OS_{1,2}-\text{min}}$) represent the high and low magnitude of switch (S_2) current as illustrated in Fig. 3. From Figure 3, it comes that D_2=0.22, I_{OS_2}=7.565 and $\Delta I_{OS_{1,2}}$=0.965, which are substituted in Eq. (8), then the total current conduction and conduction loss of power sharing switch ($S_{1,2}$) are resolved in Eqs. (9)-(10):

$$I_{S_{1,2}}^2 = 12.58\,\text{A} \tag{9}$$

$$P_{\text{cond}-S_{1,2}} = 12.58 \cdot 0.069 = 0.90\ \text{W}. \tag{10}$$

2.2.3. TOBB converter inductor losses (L_1)

($I_{OL_1-\text{max}}$) and ($I_{OL_1-\text{min}}$) represent the maximum and minimum amplitude of inductor (L_1 current as illustrated in Fig. 4. It illustrates clearly that D_{L_1}=0.67, I_{OL_1}=0 and ΔI_{OL_1}=5.25 values are substituted in Eq. (9), the total current conduction and power loss of inductor (L_1)are resolved in Equations (11) and (12):

$$I_{L_1}^2 = 1.38\,\text{A} \tag{9}$$

$$PL_{L_1} = 1.38 \cdot 0.9 = 1.242\ \text{W}. \tag{10}$$

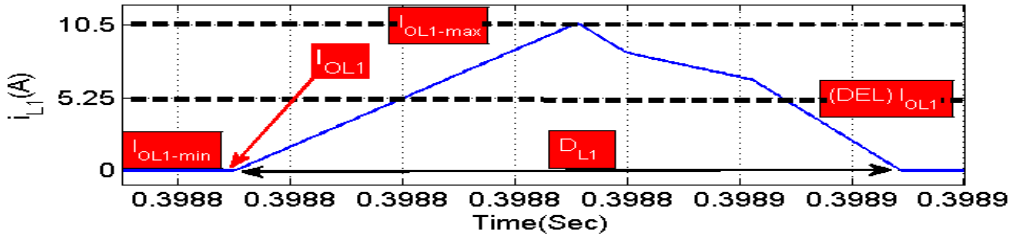

Fig. 4 – Open waveform during the conduction of inductor (L_1).

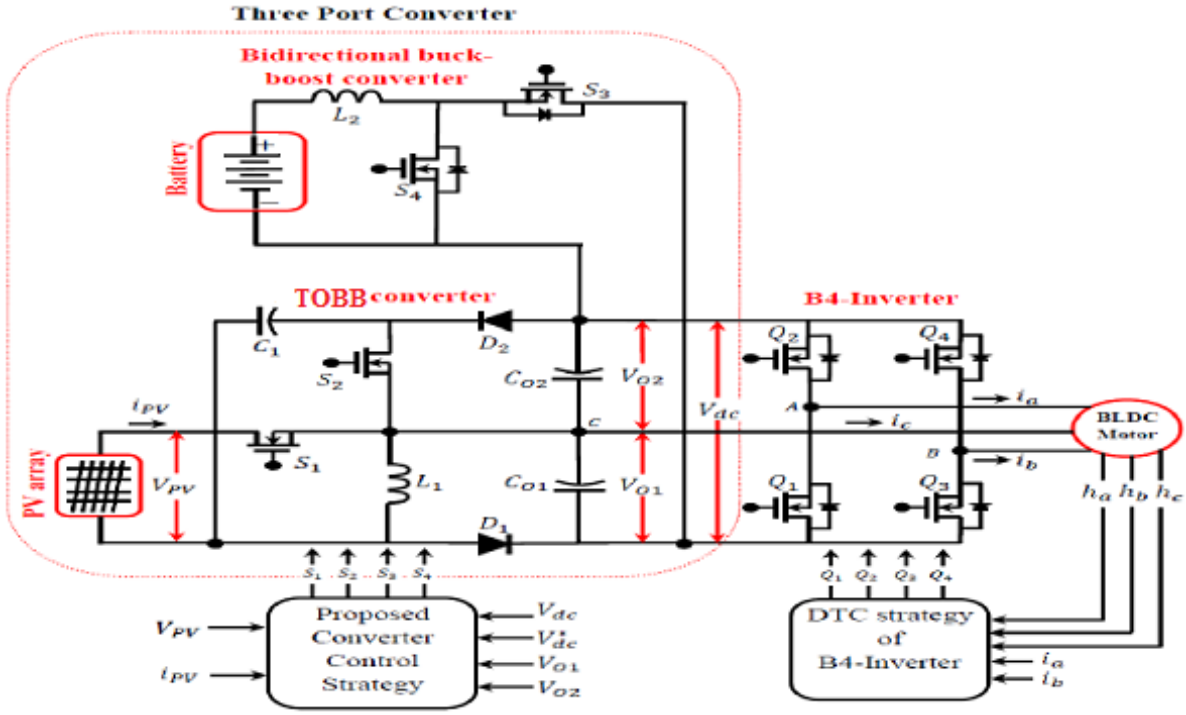

Fig. 5 – Proposed single-stage standalone PV battery powered BLDC drive.

3. RESULTS AND DISCUSSIONS

3.1. Implementation of single stage standalone supply system for BLDC drive using simulation and experimental

The simulation parameters for TOBB converter are shown in Table 1.

Table 1

Simulation parameters for TOBB converter

Components and symbols	**Parameters**
Input inductor (L_1)	389.4 μH
Intermediate Capacitor (C_1)	50 μF
Output capacitors (C_{O1}, C_{O2})	1000 μF, 100 V
Operating switching frequencies (F_{sw}) of switches	S_1=5 kHz, S_2=10 kHz
Load resistances (R_1, R_2)	28 Ω

3.2. Symmetrical output voltage control of TOBB converter

To verify the symmetrical performance of TOBB converter, input dc voltage source is considered as (V_{in}=18 V) as shown in Fig. 6a. The output voltages of the TOBB converter are desired to be regulated on

(V_{01}=18 V, V_{O2}=30 V, i.e. V_T=48 V). Consequently, the total output voltage and total power are desired to be regulated on V_T=48 V) and (P_T=40 W). Moreover, load resistances (R_1=R_2=28 ohm) are considered for symmetrical condition.

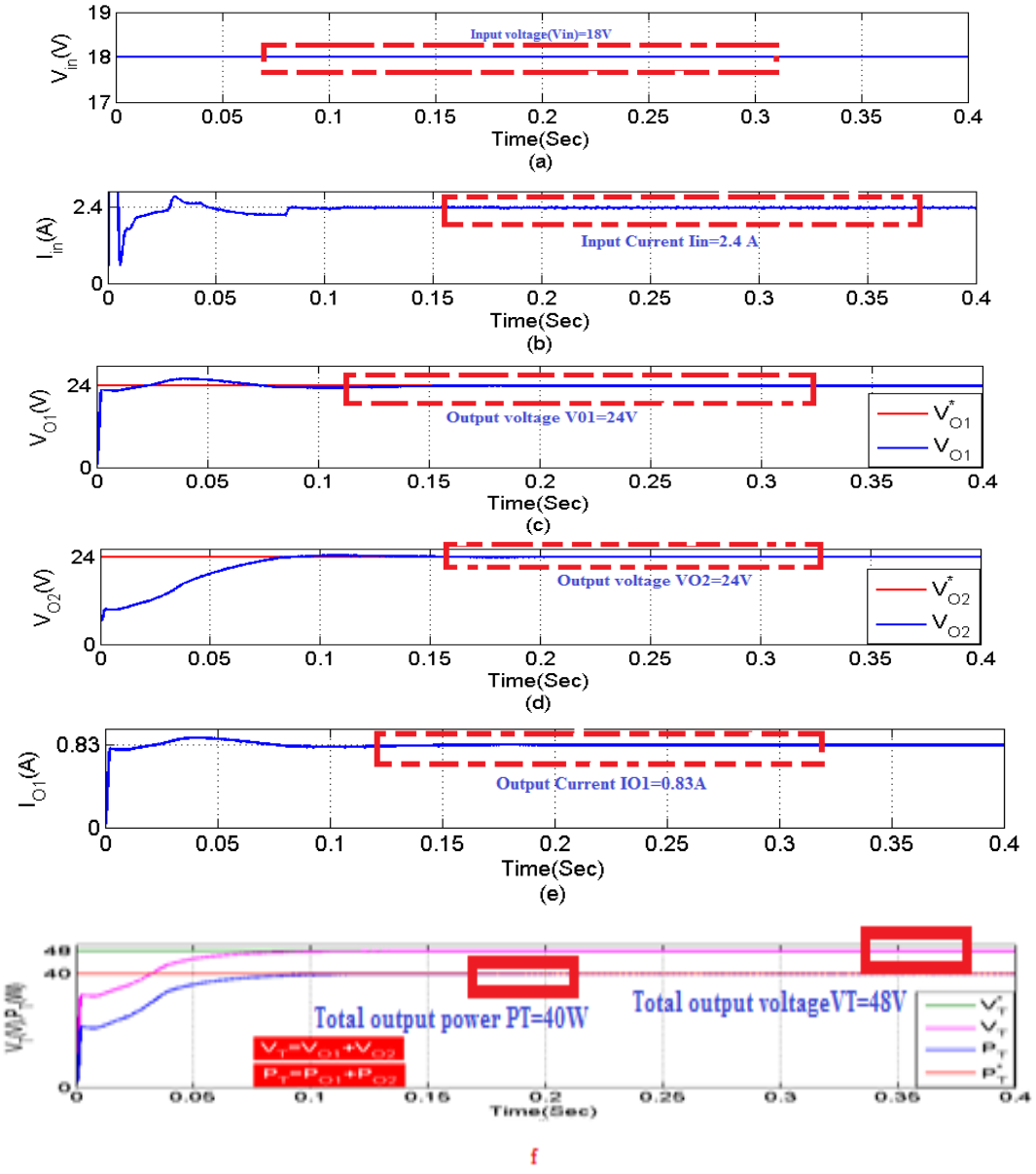

Fig. 6 – Performance of TOBB converter under symmetrical voltage condition.

In 0.4 second, a step change is generated on solar irradiation from 1000 W/m^2 to 400 W/m^2 as shown in Fig. 6a. Due to change in environmental condition panel, power is reduced from 450 W to 130 W respectively as shown in Fig. 6b. The BLDC of power rating 300 W (rated speed = 1500 rpm, rated DC voltage = 300 V, rated torque = 1.2 Nm and number of poles = 4) is taken as the load port of the proposed system. The rated power of BLDC (load power) is 300 W and rotor speed is maintained at 1500 Rpm as shown in Figs. 6c and 6f respectively. The required load power of 160 W at low irradiation case (400 W/m^2) is efficiently extracted from the battery. Similarly, the surplus power of solar module (140 W) at maximum irradiation case (1000 W/m^2) is efficiently stored in the storage battery according to the command of battery management unit shown in Fig. 6d. As can be seen from the Fig. 6d, the negative sign represents that the battery obtains the energy from the panel; consequently the positive sign indicates that the storage battery provides energy to the load. SOC is indicated in Fig. 6e.

The evaluation of the performance of the proposed system under solar dynamics is shown in Fig. 7. The sudden change in torque, the ripple is reduced so vibration in motor is reduced in proposed TOBB, output voltage are shown in Fig. 8 with the compared to conventional single output.

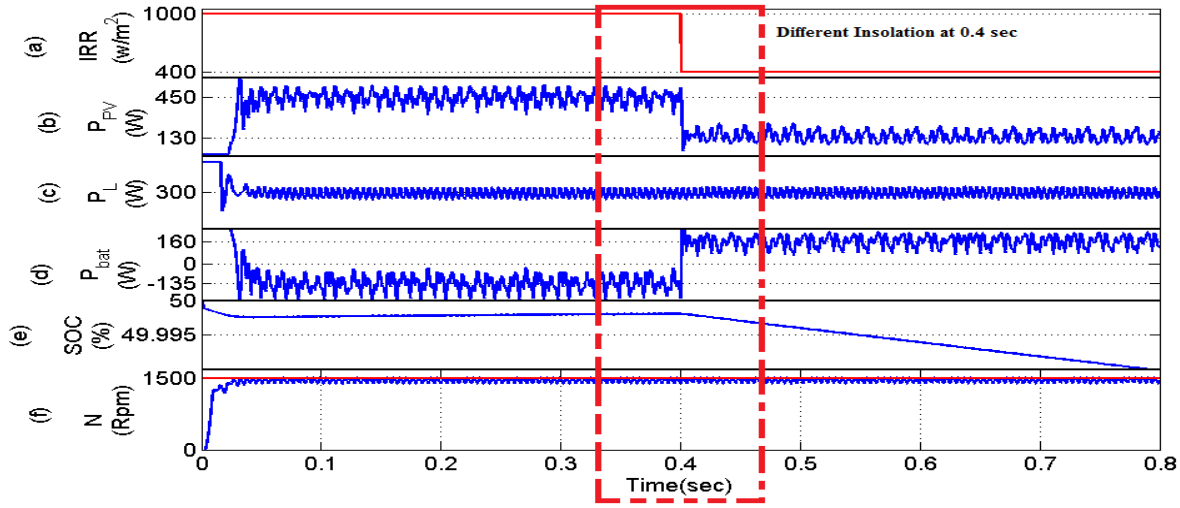

Fig. 7 – Performance of proposed two output buck boost converter employed B4-Inverter fed BLDC drive under dynamics of solar irradiation.

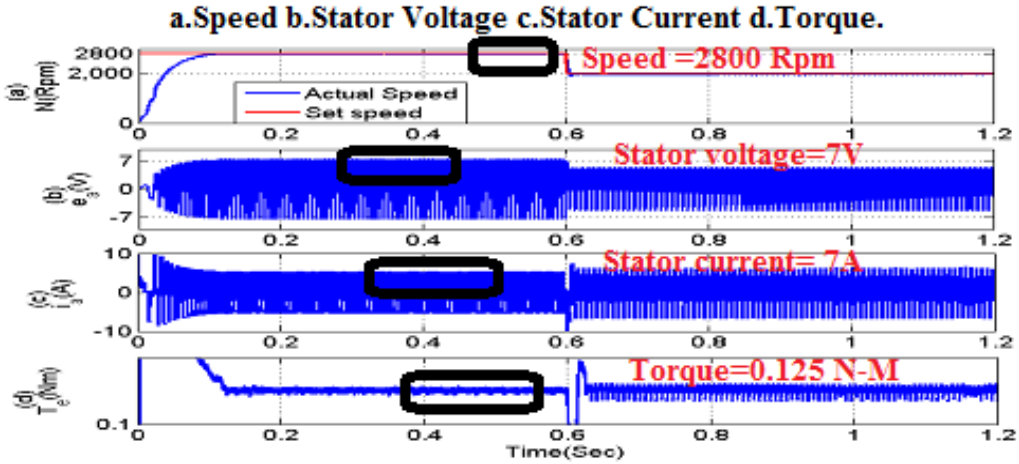

Fig. 8 – Performance of proposed multi output buck boost converter employed B4-Inverter fed BLDC drive under dynamics of solar irradiation.

3.3. Simulated comparison of two conventional converter with the proposed TOBB

To identify the limitations of conventional converters [13-15], the output voltages of the conventional converters are desired to be regulated on (C_{01}=24 V, C_{O2}=24 V, i.e, V_T=48 V) from 0 to 0.4 s. After 0.4 s, the output voltages are desired to be regulated on (V_{01}=18 V, V_{O2}=30 V, i.e. V_T=48 V) respectively as shown in Figs. 9a and 9b. For this analysis input DC voltage source is considered to be 18 V and load resistances are considered to be (R_1=R_2=28 ohm). Observing from Figs. 9a and 9b conventional converters (Nami et al. (2010) and Boora et al. (2011)) output voltages (C_{01}=24 V, C_{O2}=24 V, i.e. V_T=48 V) are regulated very well at symmetrical condition. Therefore, TOBB converter follows the reference voltages at both symmetrical and asymmetrical conditions as shown in Fig. 10.

The proposed TOBB converter topologies are compared with respect to their component count, type of conversion, possibility of output voltage control, switching states and driver circuit complexity. The Performance Comparison of the conventional and proposed TOBB converters with various objects is shown in table. The hardware component selection is shown in Table 3.

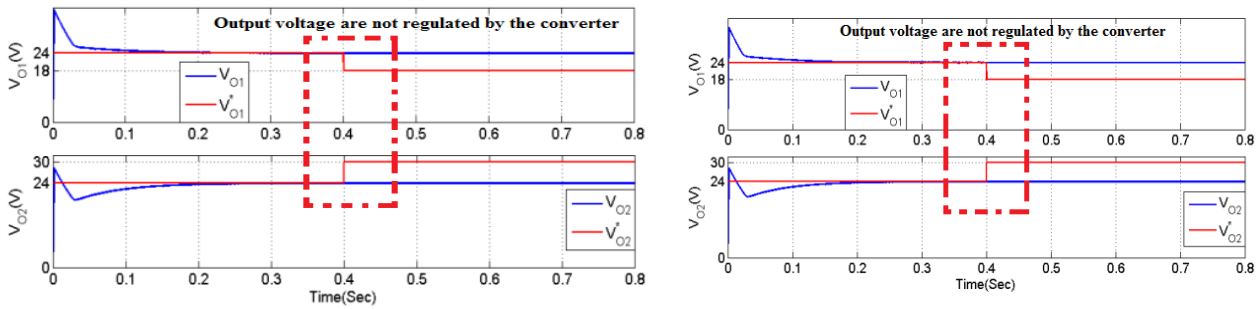

(a) (b)

Fig. 9 – a) Performance of Sathish Kumar et al. (2017) converter when $V_{01} < V_{O2}$; b) performance of Boora et al. (2011) converter.

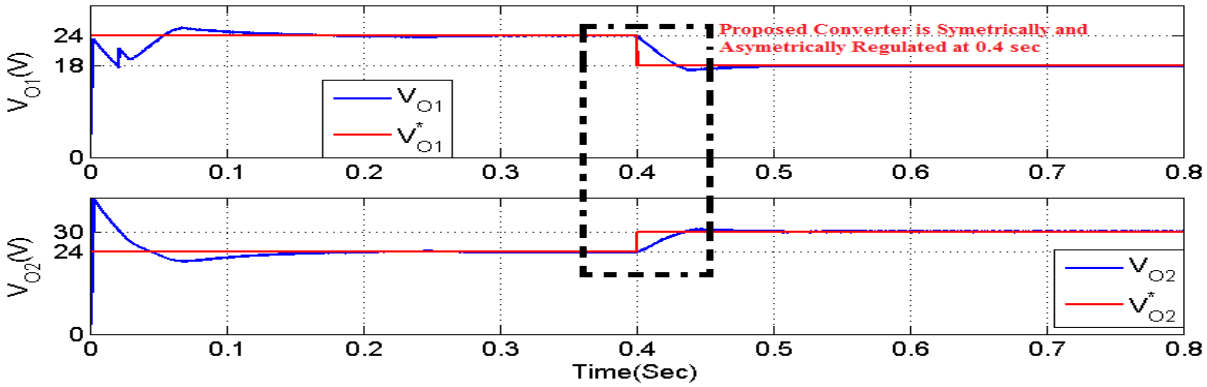

Fig. 10 – Performance of TOBB converter.

Table 2

Performance comparison of the conventional and proposed TOBB converters with various objects and comparison chart

Various Dual output converters

Objects	Converter presented by Nami et al. (2010)	Converter presented by Boora et al. (2011)	Proposed TOBB converter
Total number of Switches	2	3	2
Total number of Diodes	2	3	2
Total number of Capacitors	2	2	3
Total number of Inductors	1	1	1
Total number of components	7	9	8
Type of conversion	$V_T > V_{in}$ (step-up)	$0 > V_T > V_{in}$ (both step-up and step-down)	$0 > V_T > V_{in}$ (both step-up and step-down)
Possibility of output voltage control	$V_{O2} < (V_T/2$ or $V_{01})$	$V_{O2} < (V_T/2$ or $V_{01})$	$(V_{01}$ or $V_{O2}) < V_T$
Switching states complexity	Simple	Complex	Simple

The prototype system has been developed using the explained above method and tested in the laboratory output voltage are shown in Fig. 12. The overall system is controlled by a dsPIC30F4011 Digital Signal controller. The driver circuits are most widely used for driving the power switches like Metal-Oxide-Semiconductor Field-Effect Transistor (MOSFET) and Insulated-Gate Bipolar Transistor (IGBT).

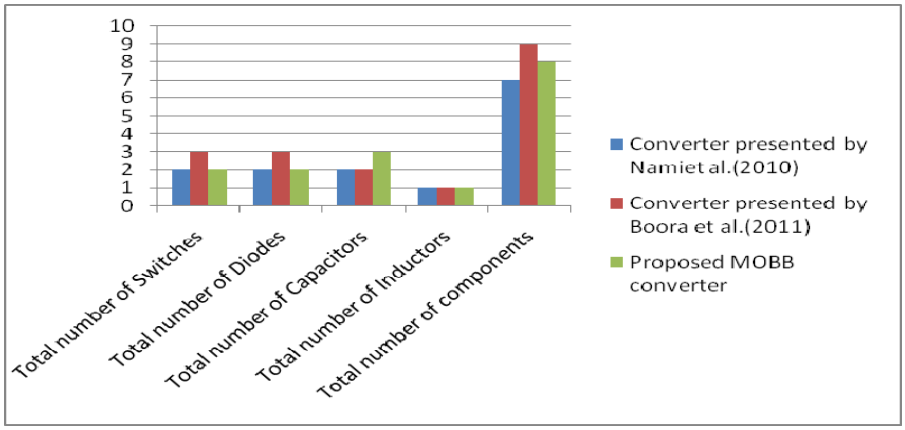

Fig. 11 – Graphical representation of Table 2 data.

Table 3

TOBB converter B4-Inverter fed BLDC motor driver components specification

Sl No.	Objects	Values
1	DC power source 1	16.6 V, 0.72 A and 12 W
2	DC power source 2	16.9 V, 4.38 A and 74 W
3	Battery power source	12 V, 7.4 Ah and 88.8 Wh
4	TPC output voltage	48 V
5	TPC output current	0.83 A
6	TPC output power	40 W
7	Rated BLDC motor power (Torque = 0.125 Nm, Speed = 2800 Rpm, DC link voltage = 24V, number of poles = 8)	39 W

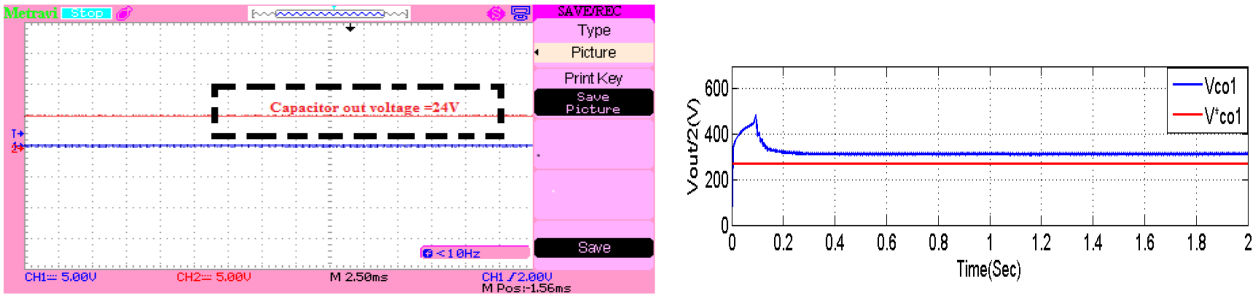

Fig. 12 – Experimental and simulation output of V_{o1}, C_{01}.

The BLDC drive using experimental hardware is shown in Fig. 13.

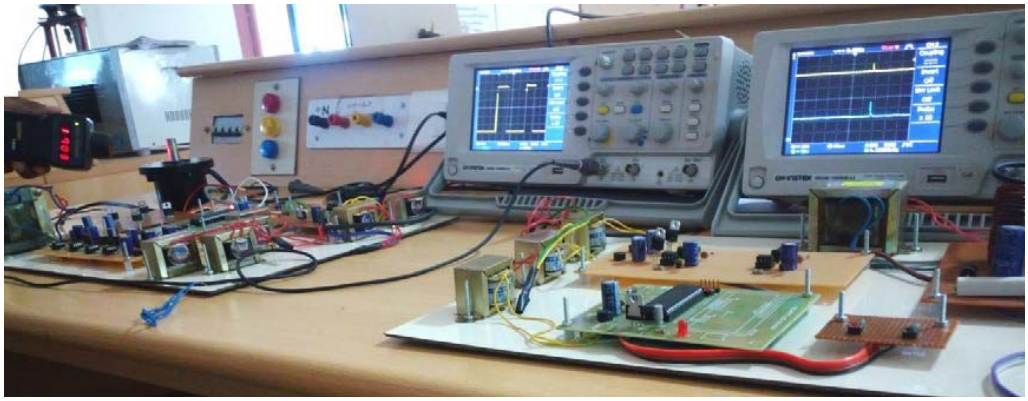

Fig. 13 – Prototype test setup of BLDC drive with different speeds.

4. CONCLUSION

The present research has proposed an enhanced Two-output BB converter based on B4-Inverter fed BLDC drive system, which is evaluated through MATLAB Simulation and experimental setup, is carried out successfully. The Two-output BB converter based PV battery standalone system is nominal compared to the existing individual Two-output systems. It also includes the minimization of power losses, switching failures in the inverter and replacement B6-Inverter with B4-inverter. The vibration and shock are sensed in the Brushless DC motor drive by accelerometer an electromechanical device and the components efficiency, losses of the proposed circuit are accurately analysed. A Matlab platform and hardware model of Two-output output Buck-Boost converter is developed for various effective environment used for industrial and agricultural applications

REFERENCES

1. Kashif ISHAQUE. Zainal SALAM, *A deterministic particle swarm optimization maximum power point tracker for PV system under partial shading condition*, IEEE Transactions on Industrial Electronics, **60**, *8*, pp. 3195–3206, 2013.
2. A.A. GHONEIM, *Design optimization of PV powered water pumping systems*, Energy Conversion and Management, **47**, *11-12*, pp. 1449–1463, 2006.
3. S.A.KH. MOZAFFARI NIAPOUR, S. DANYALI, M.B.B. SHARIFIAN, M.R. FEYZI, *BLDC drives supplied by PV power system based on Z-source inverter and FL-IC MPPT controller*, Energy Conversion and Management, **52**, *8-9*, pp. 3043–3059, 2011.
4. J. GAO, Y. HU, *Direct self-control for BLDC drives based on three-dimensional coordinate system*, IEEE Transactions on Industrial Electronics, **57**, *8*, pp. 2836–2844, 2010.
5. J. FANG, X. ZHOU, G. LIU, *Precise accelerated torque control for small inductance BLDC*, IEEE Transactions Power Electronics, **28**, *3*, pp. 1400–1412, 2013.
6. H. TAO, J. DUARTE, M. HENDRIX, *Three-port triple-half-bridge bidirectional converter with zero-voltage switching*, IEEE Transactions Power Electronics, **23**, *2*, pp. 782–792, 2008.
7. V.A.K. PRABHALA, D. SOMAYAJULA, M. FERDOWSI, *Power sharing in a double-input buck converter using dead-time control*, Proceedings of 2009 IEEE Energy Conversion Congress and Exposition, 2009, pp. 2621–2626.
8. Z. LI, O. ONAR, A. KHALIGH, E. SCHALTZ, *Design and control of a multiple input DC/DC Converter for battery/ultra capacitor based electric vehicle power system*, Proceedings of 2009 Twenty-Fourth Annual IEEE Applied Power Electronics Conference and Exposition, 2009, pp. 591–596.
9. S.M. DEHGHAN, M. MOHAMADIAN, A. YAZDIAN, F. ASHRAFZADEH, *Two-output input Two-output-output Z-source inverter*, IEEE Transactions Power Electronics, **25**, *2*, pp. 360–368, 2010.
10. O.C. ONAR, A. KHALIGH, *A novel integrated magnetic structure based DC/DC converter for hybrid battery/ultra capacitor energy storage systems*, IEEE Transactions Smart Grid, **3**, *1*, pp. 296–308, 2012.
11. K.D. HOANG, Z.Q. ZHU, M.P. FOSTER, *Influence and compensation of inverter voltage drop in direct torque-controlled four-switch three-phase PM brushless AC drives*, IEEE Transactions of Power Electronics., **26**, *8*, pp. 2343–2357, 2011.
12. Rajan KUMAR, Bhim SINGH, Ambrish CHANDRA, Kamal AL-HADDAD, *Solar PV array fed water pumping using BLDC drive with Boost-Buck converter*, 2015 IEEE Energy Conversion Congress and Exposition (ECCE), October 20-24, 2015, pp. 5741–5748.
13. S. SHANMUGAM, M. RAMACHANDRAN, K. KANAGARAJ, A. LOGANATHAN, *Sensorless control of four-switch inverter for brushless DC motor drive and its simulation*, Circuits and Systems, **7**, *6*, pp. 726–734, 2016.
14. Sathish KUMAR SHANMUGAM, Arumugam SENTHILKUMAR, *Design and implementation of DC source fed improved dual-output buck-boost converter for agricultural and industrial applications*, Journal of Vibroengineering, **19**, *8*, pp. 6433–6454, December 2017; DOI: https://doi.org/10.21595/jve.2017.19228.
15. Sathish KUMAR SHANMUGAM, Arumugam SENTHILKUMAR, *Implementation of solar photovoltaic array and battery powered enhanced DC-DC converter using B4-inverter fed brushless DC motor drive system for agricultural water pumping applications*, Journal of Vibroengineering, **20**, *2*, pp. 1214–1233, 2018, https://doi.org/10.21595/jve.2018.19449.

Received April 7, 2018